SUPERCONDUCTIVITY

Anomalously strong near-neighbor attraction in doped 1D cuprate chains

Zhuoyu Chen[1,2,3]†, Yao Wang[4]†, Slavko N. Rebec[1,2,3], Tao Jia[1,3,5], Makoto Hashimoto[6], Donghui Lu[6], Brian Moritz[1], Robert G. Moore[1,7], Thomas P. Devereaux[1,3,8]*, Zhi-Xun Shen[1,2,3,5]*

In the cuprates, one-dimensional (1D) chain compounds provide a distinctive opportunity to understand the microscopic physics, owing to the availability of reliable theories. However, progress has been limited by the challenge of controllably doping these materials. We report the synthesis and spectroscopic analysis of the 1D cuprate $Ba_{2-x}Sr_xCuO_{3+\delta}$ over a wide range of hole doping. Our angle-resolved photoemission experiments reveal the doping evolution of the holon and spinon branches. We identify a prominent folding branch whose intensity fails to match predictions of the simple Hubbard model. An additional strong near-neighbor attraction, which may arise from coupling to phonons, quantitatively explains experiments for all accessible doping levels. Considering structural and quantum chemistry similarities among cuprates, this attraction may play a similarly important role in high-temperature cuprate superconductors.

Strong correlations in electronic materials such as high-temperature cuprate superconductors lead to complex properties that have been a central challenge in condensed matter physics (1). So far, there remains no exact solution of many-body Hamiltonians in two or more dimensions, making a quantitative comparison between theory and experiment a challenge. A promising route to improved understanding may be through the analysis of one-dimensional (1D) systems: The reduced dimension enables exact solutions of microscopic Hamiltonians like the Hubbard model and low-energy field theory without bias. Such possibilities have been recognized in theory, but progress has been hindered by the lack of suitable experimental material systems.

In a 1D system, strong correlations manifest as so-called spin-charge separation (2–7). As schematized in Fig. 1A, a photoinduced hole fractionalizes into a "spinon" and a "holon," carrying spin and charge, respectively, giving rise to spectral branches with different propagation velocities. For half-filled d^9 systems, such spin-charge separation along with a Mott gap (Fig. 1B) has been confirmed by angle-resolved photoemission spectroscopy (ARPES) (4–6). However, the simplicity of the spectrum in the undoped case and the lack of information on interactions between doped carriers make it difficult to establish a connection to underlying microscopic models. In particular, it remains undetermined whether fundamental Hamiltonians, like the Hubbard or t-J models, contain all of the essential ingredients for general cuprate properties, including d-wave superconductivity in 2D. To address this question, a doping-dependent study of a 1D cuprate chain compound would be beneficial. However, controllably doped 1D cuprate systems remain elusive after more than two decades of effort (4–6).

We achieved a wide range of hole doping in a corner-sharing cuprate chain by synthesizing $Ba_{2-x}Sr_xCuO_{3+\delta}$ (BSCO, whose lattice structure is shown in Fig. 1C). Thin films were grown with a recently developed ozone-reactive molecular beam epitaxy (MBE) system connected in situ to ARPES beamline 5-2 at the Stanford Synchrotron Radiation Lightsource (SSRL). Atomic layer-by-layer growth in purified ozone was monitored in real-time via in situ reflective high energy electron diffraction (RHEED; fig. S1, B and C) (8). A mixture of isovalent Sr and Ba facilitates the tuning of in-plane lattice constants to mitigate mismatches with $SrTiO_3$ substrates (9). Orthorhombic BSCO on cubic $SrTiO_3$ forms twinned domains with different chain orientations (fig. S1, D and E). In different domains, chain directions are perpendicular to each other and parallel to the substrate
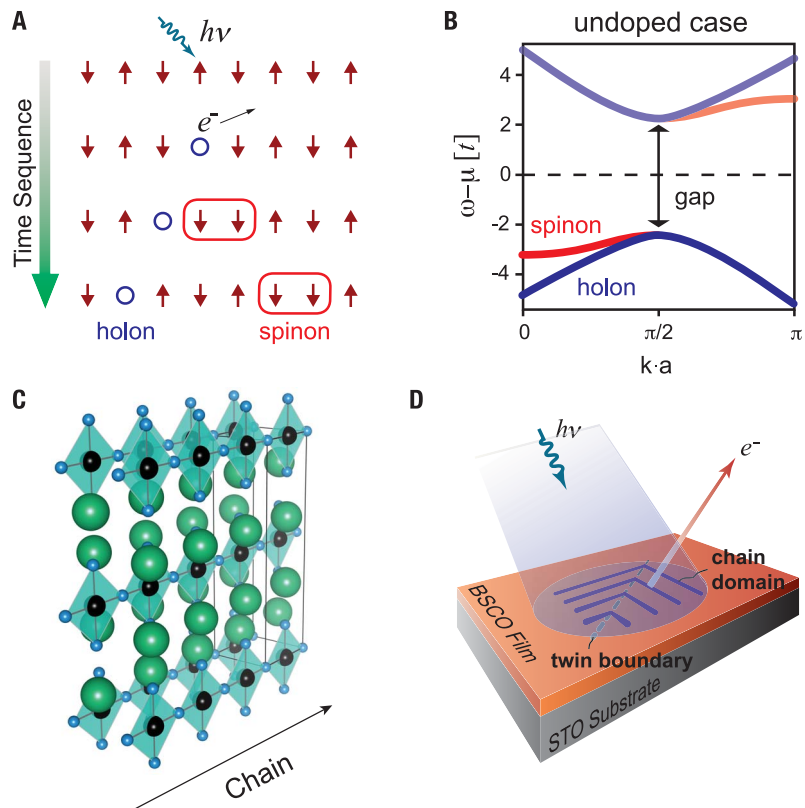
[1]Stanford Institute for Materials and Energy Sciences, SLAC National Accelerator Laboratory, Menlo Park, CA 94025, USA. [2]Department of Applied Physics, Stanford University, Stanford, CA 94305, USA. [3]Geballe Laboratory for Advanced Materials, Stanford University, Stanford, CA 94305, USA. [4]Department of Physics and Astronomy, Clemson University, Clemson, SC 29631, USA. [5]Department of Physics, Stanford University, Stanford, CA 94305, USA. [6]Stanford Synchrotron Radiation Lightsource, SLAC National Accelerator Laboratory, Menlo Park, CA 94025, USA. [7]Materials Science and Technology Division, Oak Ridge National Laboratory, Oak Ridge, TN 37831, USA. [8]Department of Materials Science and Engineering, Stanford University, Stanford, CA 94305, USA.
*Corresponding author. Email: tpd@stanford.edu (T.P.D.); zxshen@stanford.edu (Z.X.S.)
†These authors contributed equally to this work.

Fig. 1. Strongly correlated antiferromagnetic (AFM) cuprate chain. (A) Schematic of an example photoemission process in a 1D AFM chain. Red arrows, blue circles, and red rounded rectangles correspond to spin-full electrons, holons, and spinons, respectively. The green arrow represents the arrow of time. (B) Schematic diagram of the spectral dispersion relation for an undoped chain. Blue and red solid lines correspond to the holon and spinon branches, respectively. (C) The lattice structure of $Ba_{2-x}Sr_xCuO_{3+\delta}$. Green, blue, and black balls correspond to Ba/Sr, O, and Cu atoms, respectively. (D) Schematic of sample setup for photoemission. The BSCO film on the $SrTiO_3$ (STO) substrate is twinned with chain domains smaller than the beam spot.

surface (Fig. 1D). All ARPES data shown below were collected for temperatures lower than 20 K with 65-eV photons, from one single 2.5 unit-cell sample (equivalent to 5 $Ba_{1-x/2}Sr_{x/2}O$-CuO-$Ba_{1-x/2}Sr_{x/2}O$ layers) with nominal x = 0.16 measured by quartz crystal microbalance. Doping by interstitial oxygen was controlled via ozone and vacuum annealing series (10).

Figure 2, A1 to A6, present the ARPES Fermi surface maps with controlled hole doping from 9% up to 40%. The two perpendicular Fermi surfaces indicate simultaneous photoelectron detection from both sets of domains, as mentioned above. Within each set, the lack of transverse dispersion in the spectral dis-

tribution demonstrates the highly 1D nature of the chains. Figure 2, B1 to B6, exhibit the energy-momentum spectra of cuts along the Brillouin zone edge. These cuts are located at a position where the spectral weight from one set of domains is minimized, enabling analysis of the spectra from chains with a single orientation. Note that features at higher binding energies beyond 1.2 eV are compromised by nonbonding oxygen band intensities (11). Figure 2, C1 to C6, show the corresponding second derivatives to highlight the quasiparticle features.

Comparison to cluster perturbation theory (CPT) simulations for the single-band Hubbard model (12, 13), displayed in Fig. 2, D1 to D6,

allows for the identification of the following spectral features: (i) The highest-intensity features correspond to main holon branches (blue dashed lines with "h" in B1 and C1) crossing the Fermi level E_F at the Fermi momentum k_F; (ii) spinon branches (red dashed lines with "s" in B1 and C1), which flatten near $k_{||}$ = 0 and merge into the main holon branches for higher momenta. These features agree with previous observations in undoped, parent materials (4–6). The persistence of spin-charge separation up to 40% doping agrees with predictions from the single-band Hubbard model, showing that correlation effects remain very strong in 1D, even for higher dopings (14). By fitting the
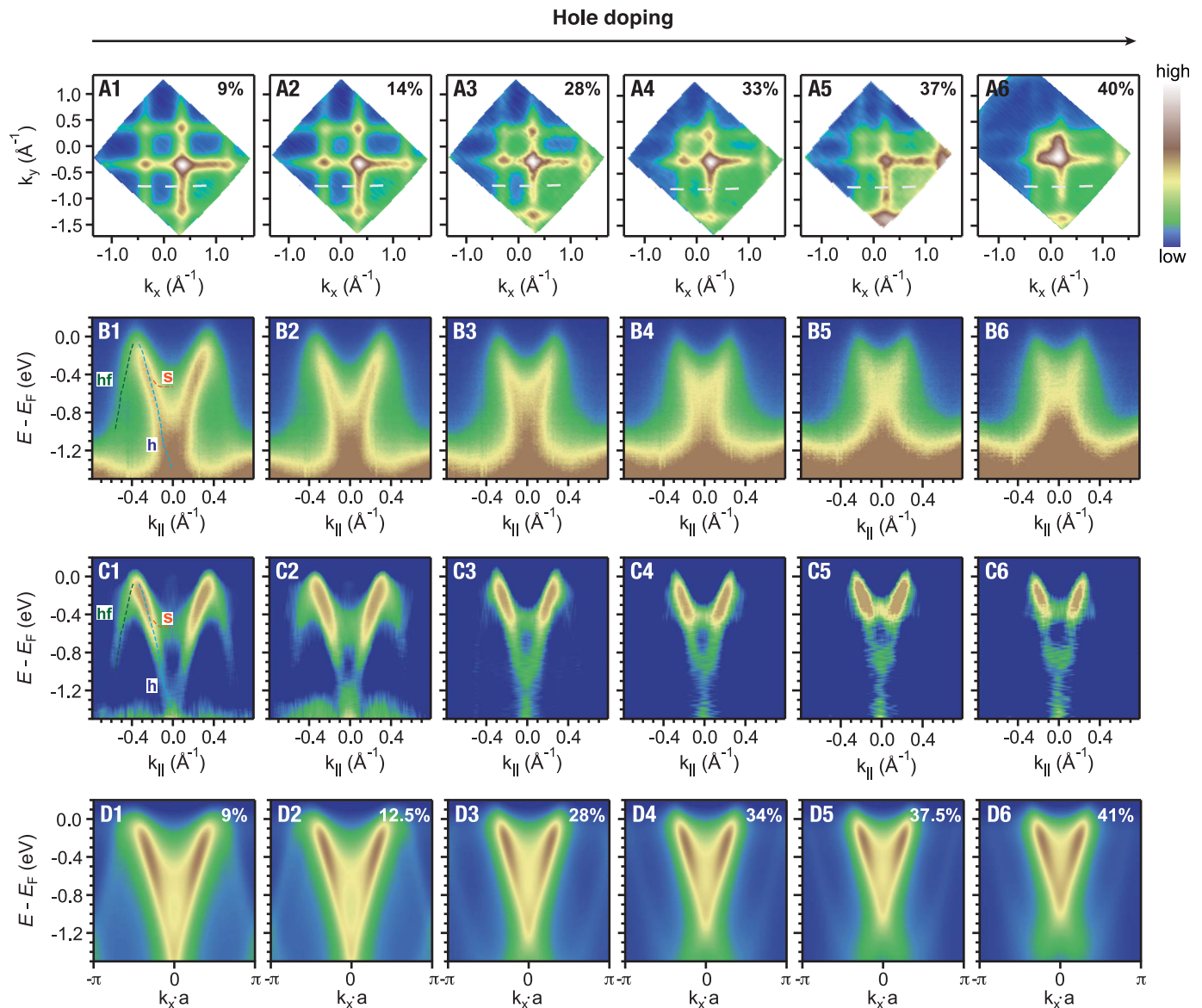
Hole doping

Fig. 2. Hole doping series of ARPES spectra. (**A1** to **A6**) Fermi surface maps with different hole doping levels. Black squares show the first Brillouin zone of the STO substrate. (**B1** to **B6**) Measured ARPES spectra taken along the cuts shown with white dashed lines in (A1) to (A6). (**C1** to **C6**) Second derivatives of energy distribution curves and momentum distribution curves are summed with sign reversed for comparison. Dashed blue, red, and green lines in (B) and (C) indicate the location of the holon ("h"), spinon ("s"), and holon folding ("hf") features. (**D1** to **D6**) Spectral function simulation results based on 16-site cluster perturbation theory (CPT) with varied corresponding hole doping levels.

doping-dependent spinon and holon binding energies at $k_{||} = 0$ (figs. S2 and S3), we obtained Hubbard model parameters $U = 8t$ and $t = 0.6$ eV, with an estimated $J = 4t^2/U = 0.3$ eV, consistent with earlier results (6, 7).

In contrast to the observations in undoped compounds (4–6), an additional feature at $|k| > |k_F|$, denoted by "hf" in Fig. 2, B1 and C1, fades rapidly with doping, as shown more directly in the momentum distribution curves (MDCs) for 9%, 14%, and 33% doping (see subdominant peaks in Fig. 3, A, B, and C, respectively). As illustrated in Fig. 3D and in comparison with theory (14–16), the holon dispersion inherited from the undoped cuprate splits into two branches at k_F for doped systems: one folding directly at E_F and k_F represented in green [hereafter the holon folding (hf) branch], and the other crossing E_F and bending back at a larger momentum $2\pi - 3k_F$ (hereafter the $3k_F$ branch) as an extension of the main holon branch. Note that the term "folding" here is simply a description of the spectral feature rather than suggesting existence of translational symmetry breaking. The Lorentzian fitting of our MDCs yields the peak positions plotted in Fig. 3E and confirms the observed prominent "hf" spectral feature as being the holon folding branch (green). The presence of the hf branch agrees with predictions using the single-band Hubbard (14–16) or t-J models (17, 18), previously attributed to a holon-holon interaction mediated by the spin superexchange and intrinsic in these models. This interaction occurs in the lowest-order t/U expansion as an attractive form with the magnitude $\sim J/4 \sim 0.1t$ (19).

Despite a consistency with the basic dispersion, we find that the simple Hubbard model is fundamentally deficient in accurately addressing additional spectral features. As evident in the MDCs shown in Fig. 4A, the Hubbard model prediction (second curve from top) shows that the relative intensity of the hf feature is rather weak compared to the $3k_F$ branch, whereas the experimental observation is the opposite. This implies that realistic holon-holon attractive interaction is not adequately described by the spin superexchange. To reproduce the experimental spectra, we find that a sizable attractive near-neighbor Coulomb interaction V must be introduced to the Hubbard Hamiltonian (19). Figure 4A displays the MDCs extracted from simulations with different V values from positive (repulsive) to negative (attractive): The near-neighbor attractive Coulomb interaction enhances the spectral weight of the hf branch and suppresses the $3k_F$ branches. We conclude that a strong holon-holon attraction $V \approx -1.0t$ matches well with the experimental spectra (bottom curve) and explains why the $3k_F$ branch is not found in experiment. Note that in principle such attraction in 1D primarily affects the charge degree of freedom; thus, the chemical potential is pinned by the
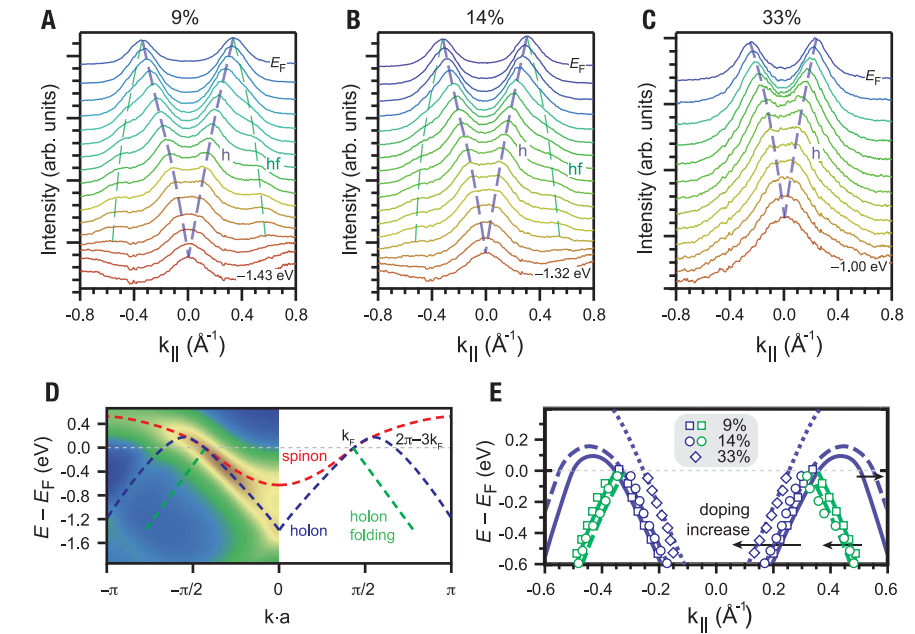

Fig. 3. Identification of the holon folding. (**A** to **C**) MDCs for varied energies at 9, 14, and 33% hole doping. Purple and green dashed lines are guides to the eye for the holon (h) and the holon folding (hf) branches. (**D**) CPT simulation based on single-band Hubbard model without Fermi-Dirac suppression above E_F for the 12.5% doping case, shown in the color-scale plot. Dashed lines with different colors track the traces of different branches as revealed by the CPT simulation. Note that the holon folding feature (faint white) is relatively weak and barely visible in the color-scale plot for the CPT simulation of pure Hubbard model without additional terms. (**E**) Peak positions extracted from MDCs for different dopings (squares: 9%; circles: 14%; diamonds: 33%) overlaid on theoretical lines of single-band Hubbard prediction, where solid, dashed, and dotted lines correspond to increasing doping. Blue and green colors correspond to the major holon (h) and the holon folding (hf) branches, respectively. Black arrows indicate the direction of the shift for different features with increasing dopings.

spinon dispersions, unlike 2D cases where a quasiparticle gap is usually expected.

As mentioned above, the hf spectral feature fades rapidly with increasing doping, as summarized in Fig. 4B, perhaps implying a doping-dependent holon-holon attraction. Comparing both the spectral intensity and the doping level at which it vanishes (figs. S4 and S5), we find the best agreement with a (doping-independent) V between $-1.2t$ and $-0.8t$. To quantify this strong doping dependence, we extract the relative hf peak intensities with respect to the main holon-peak intensities based on Lorentzian fittings for experimental MDCs (circles in Fig. 4C); for comparison, we perform the same fitting on the simulated MDCs with $V = -1.0t$ (squares in Fig. 4C). The doping dependence of the hf peak intensity is captured for a fixed V, whose influence is renormalized by doping, such that this intensity gradually decreases and eventually disappears at $\sim 30\%$ hole doping. That is, the doping dependence is intrinsic in the calculation and does not require parameter tuning. The Coulomb interaction between electrons should always be repulsive, so the only probable origin of this effective attraction, beyond spin superexchange already accounted for in the Hubbard model, would be coupling to some

bosonic excitations. Although multiple bosonic modes may play a role in cuprates, here, we postulate that the attractive V is mediated by phonons, considering the evidence of electron-phonon coupling in a variety of cuprates (20–29).

We emphasize that this additional near-neighbor attraction is an order of magnitude stronger than the inherent attraction in the Hubbard model mediated by spin superexchange (given by $-J/4$ in the limit of $t/U \ll 1$), when considering all interactions on the same footing. This is demonstrated in Fig. 4D, in which a baseline of zero net attraction is found by using the simulated folding peak relative intensity as a phenomenological parameter and back-extrapolating it as a function of V. In the case of the Hubbard model ($V = 0$), the effective attraction is $\sim 0.1t$ above the baseline (consistent with the $J/4$ estimation), whereas the experimental case is at least $\sim 1t$ above the baseline, an order of magnitude larger. This difference implies that the single-band Hubbard model misses a sizable, attractive interaction between neighboring holes, which likely originates from electron-phonon coupling (19, 30, 31).

Considering the structural similarities among cuprates, our Hamiltonian with near-neighbor attraction should be applicable to CuO_2 planes
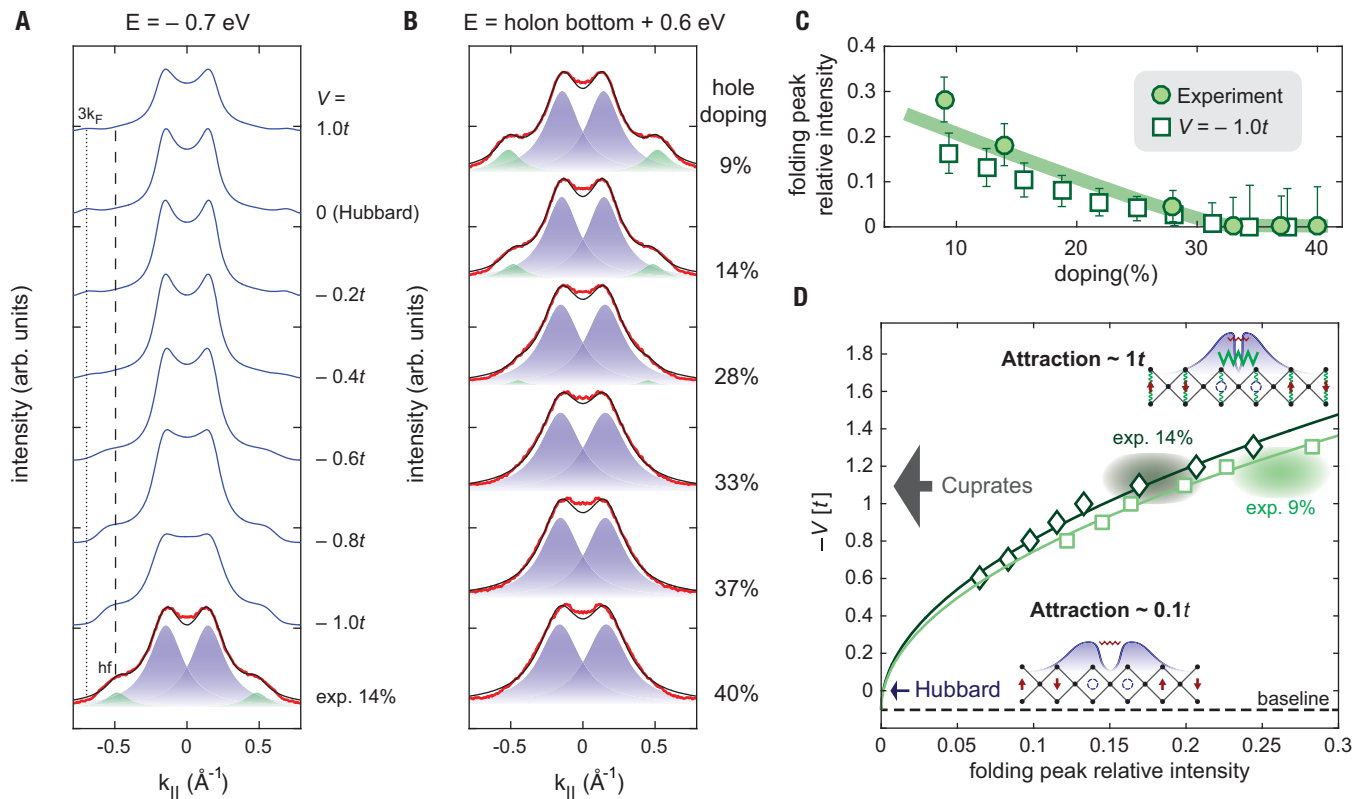
Fig. 4. Strong holon folding indicating attractive interaction beyond Hubbard model. (**A**) CPT simulation incorporating a near-neighbor interaction term V (blue curves), compared with experimental MDC at −0.7 eV below E_F for 14% doping (red curve). Black curve is a fit utilizing two Lorentzian peaks shown in blue (major) and green (hf). Vertical dashed and dotted lines mark the locations of the hf and the $3k_F$ branch peaks, respectively. Curves are shifted and scaled vertically for comparison. (**B**) Doping-dependent experimental MDCs at energies approximately 0.6 eV above the holon bottom, such that the major branch peaks have similar momenta for comparison. (**C**) Folding peak intensity relative to the major peak intensity as a function of doping (circles: experiment; squares: simulations for $V = -1.0t$). The green line is a guide to the eye.

(**D**) $-V$ as a function of CPT simulated folding peak relative intensity f as a phenomenological measure of the net near-neighbor attraction (squares: 9%; diamonds: 12.5%). The solid green curves are a fit to the data using $f = a(V - V_0)^2$, where a is a doping-dependent prefactor and V_0 represents the compensation against the effective attraction in the Hubbard model, $\sim (0.10 \pm 0.05)t$ given by the fitting. The gray shaded areas correspond to experimental points (and error bars) of 9 and 14% dopings. Insets: Schematic of holon attractions for the pure Hubbard model (lower) and the mediation by bosons (upper). In addition to the symbols introduced in Fig. 1A, green springs, blue shades, and red and green zigzags represent electron-phonon coupling, holon distributions, AFM-, and boson-mediated attractions, respectively.

and favors neighboring electron pairs. Given that the Hubbard model with strong on-site repulsive U and strong near-neighbor attractive V explains the essential physics in 1D—charge, spin, charge-charge attraction and its doping dependence—it is plausible that such an augmented Hubbard model provides a holistic picture for all cuprates, including robust d-wave superconductivity that has been elusive in all 2D Hubbard-like models.

REFERENCES AND NOTES

1. B. Keimer, S. A. Kivelson, M. R. Norman, S. Uchida, J. Zaanen, *Nature* **518**, 179–186 (2015).
2. E. H. Lieb, F. Y. Wu, *Phys. Rev. Lett.* **20**, 1445–1448 (1968).
3. J. Voit, *Rep. Prog. Phys.* **58**, 977–1116 (1995).
4. C. Kim et al., *Phys. Rev. Lett.* **77**, 4054–4057 (1996).
5. H. Fujisawa et al., *Phys. Rev. B* **59**, 7358–7361 (1999).
6. B. J. Kim et al., *Nat. Phys.* **2**, 397–401 (2006).
7. J. Schlappa et al., *Nature* **485**, 82–85 (2012).
8. Z. Liu, T. Hanada, R. Sekine, M. Kawai, H. Koinuma, *Appl. Phys. Lett.* **65**, 1717–1719 (1994).
9. D. R. Lines, M. T. Weller, D. B. Currie, D. M. Ogbome, *Mater. Res. Bull.* **26**, 323–331 (1991).
10. H. Sato, M. Naito, H. Yamamoto, *Physica C* **280**, 178–186 (1997).
11. Y. F. Kung et al., *Phys. Rev. B* **93**, 155166 (2016).
12. D. Sénéchal, D. Perez, M. Pioro-Ladrière, *Phys. Rev. Lett.* **84**, 522–525 (2000).
13. D. Sénéchal, D. Perez, D. Plouffe, *Phys. Rev. B* **66**, 075129 (2002).
14. M. Kohno, *Phys. Rev. Lett.* **105**, 106402 (2010).
15. H. Benthien, F. Gebhard, E. Jeckelmann, *Phys. Rev. Lett.* **92**, 256401 (2004).
16. A. Nocera, F. H. L. Essler, A. E. Feiguin, *Phys. Rev. B* **97**, 045146 (2018).
17. K. Penc, K. Hallberg, F. Mila, H. Shiba, *Phys. Rev. Lett.* **77**, 1390–1393 (1996).
18. K. Penc, K. Hallberg, F. Mila, H. Shiba, *Phys. Rev. B* **55**, 15475–15488 (1997).
19. See supplementary materials.
20. A. Lanzara et al., *Nature* **412**, 510–514 (2001).
21. K. M. Shen et al., *Phys. Rev. Lett.* **93**, 267002 (2004).
22. T. Cuk et al., *Phys. Rev. Lett.* **93**, 117003 (2004).
23. A. S. Mishchenko, N. Nagaosa, *Phys. Rev. Lett.* **93**, 036402 (2004).
24. H. Matsueda, T. Tohyama, S. Maekawa, *Phys. Rev. B* **74**, 241103 (2006).
25. C. Slezak, A. Macridin, G. A. Sawatzky, M. Jarrell, T. A. Maier, *Phys. Rev. B* **73**, 205122 (2006).
26. O. Gunnarsson, O. Rösch, *Phys. Rev. B* **73**, 174521 (2006).
27. Y. He et al., *Science* **362**, 62–65 (2018).
28. W. S. Lee et al., *Phys. Rev. Lett.* **110**, 265502 (2013).
29. J. J. Lee et al., *Phys. Rev. B* **89**, 041104 (2014).
30. H. Suzuura, H. Yasuhara, A. Furusaki, N. Nagaosa, Y. Tokura, *Phys. Rev. Lett.* **76**, 2579–2582 (1996).
31. S. Johnston et al., *Phys. Rev. B* **82**, 064513 (2010).
32. Z. Chen et al., Replication Data for: Anomalously Strong Near-Neighbor Attraction in Doped 1D Cuprate Chains, *Harvard Dataverse* (2021). https://doi.org/10.7910/DVN/5I1WSW.

SUPPLEMENTARY MATERIALS

Science

Anomalously strong near-neighbor attraction in doped 1D cuprate chains

Zhuoyu ChenYao WangSlavko N. RebecTao JiaMakoto HashimotoDonghui LuBrian MoritzRobert G. MooreThomas P. DevereauxZhi-Xun Shen

Exploring cuprate chains

Superconductivity in cuprates takes place in their two-dimensional (2D) layers but solving even the simplest model of interacting fermions in 2D is a challenge. The theory problem simplifies in 1D, with experiment becoming the tricky part. Chen *et al*. synthesized a cuprate that consists of parallel chains and behaves like a 1D system. Crucially, the material could be doped over a wide range of hole concentrations. The researchers showed that including a near-neighbor attractive interaction in a 1D model of interacting fermions was necessary to explain their photoemission measurements. —JS

View the article online
https://www.science.org/doi/10.1126/science.abf5174
Permissions
https://www.science.org/help/reprints-and-permissions

Use of think article is subject to the Terms of service